Supporting Information

Multiscale simulations reveal the driving forces of p53C phase separation accelerated by oncogenic mutations

Yawei Yu, Qian Liu, Jiyuan Zeng, Yuan Tan, Yiming Tang and Guanghong Wei*

Department of Physics, State Key Laboratory of Surface Physics, and Key Laboratory for Computational Physical Sciences (Ministry of Education), Fudan University, Shanghai 200438, People's Republic of China.

E-mail: ghwei@fudan.edu.cn

This supporting material contains thirteen figures (Fig. S1-S13).

Unless specified, all the results presented below are obtained using the data from three independent AA MD runs and two independent CG MD runs.

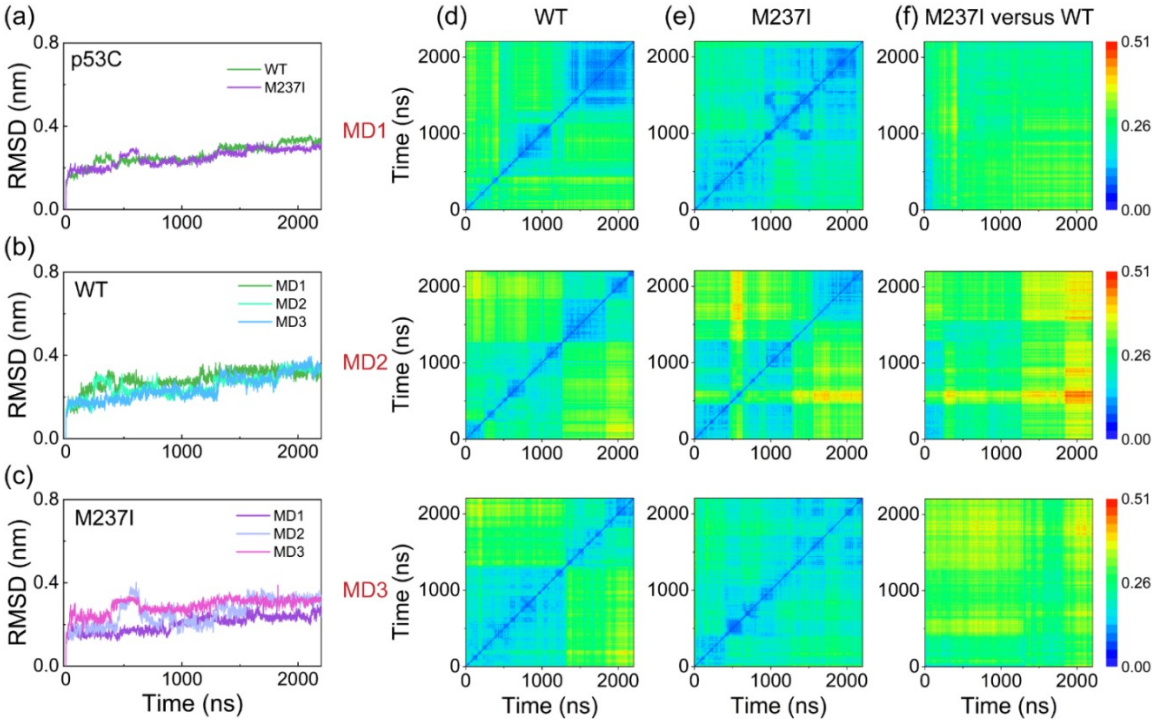

Fig. S1 (a-c) Time evolution of (a) backbone RMSD values of p53C averaged over three MD runs, (b) RMSD values of three WT MD runs, and (c) RMSD values of three M237I MD runs. (d-f) The RMSD values matrix of (d) WT, (e) M237I, and (f) M237I versus WT.

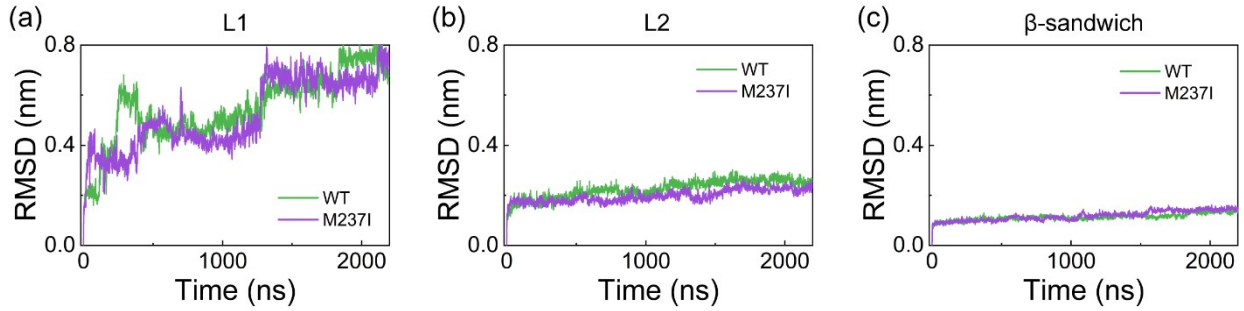

Fig. S2 (a-c) Time evolution of backbone RMSD values of (a) L1, (b) L2, and (c) β-sandwich regions averaged over three MD runs.

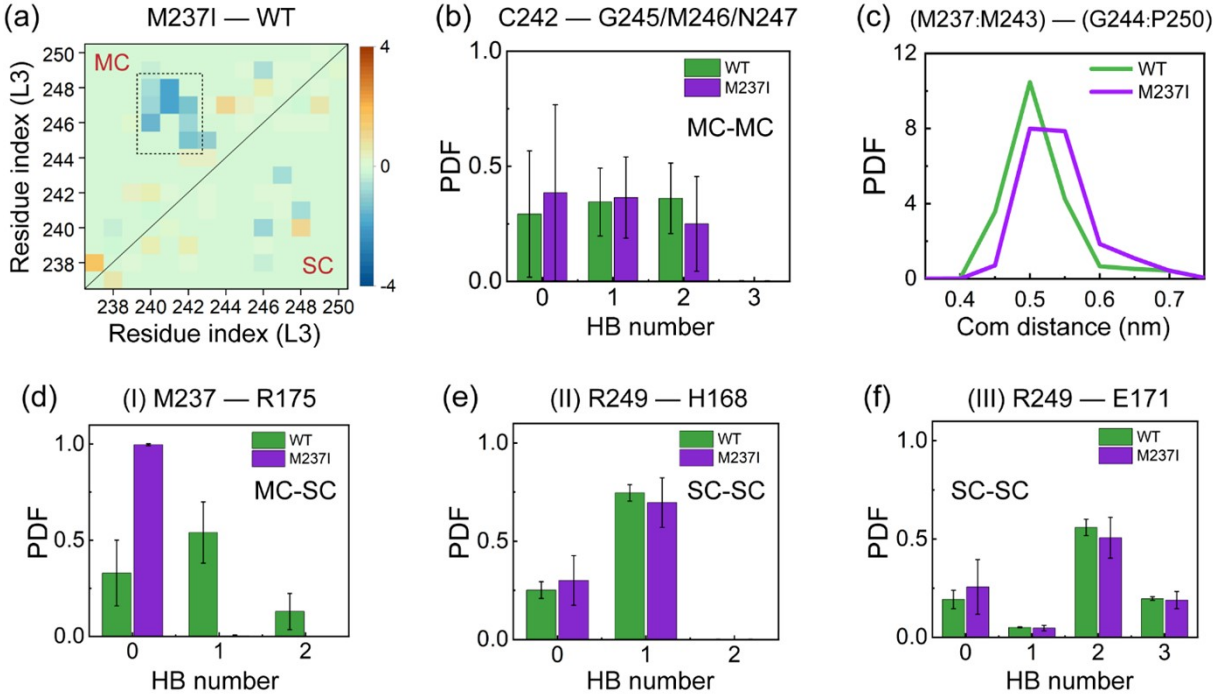

Fig. S3 (a) The differences of L3-L3 contact number map between M237I and WT (i.e. M237I minus WT, L3 residues: M237I-P250), the upper triangle region is the MC-MC interactions, the lower triangle region is the SC-SC interactions. (b) The PDF of MC-MC HB number between residues C242 and G245/M246/N247. (c) The PDF of center of mass distance between Cα atoms of N-terminal (residues M/I237-M243) and Cα atoms of C-terminal (residues G244-P250) in L3. (d-f) The PDF of HB number of residue pairs (d) M/I237-R175, (e) R249-H168, and (f) R249-E171.

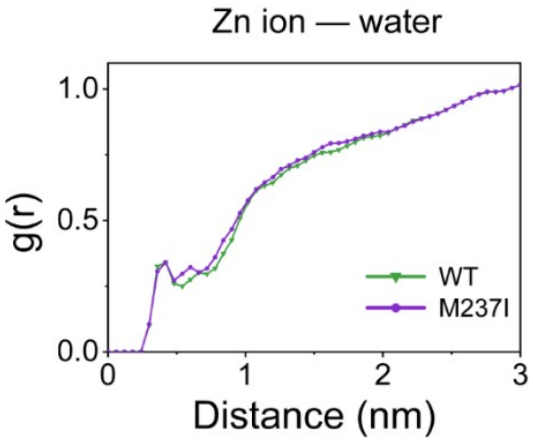

Fig. S4 The RDF between the Zn ion in p53C and the oxygen atom in water molecules.

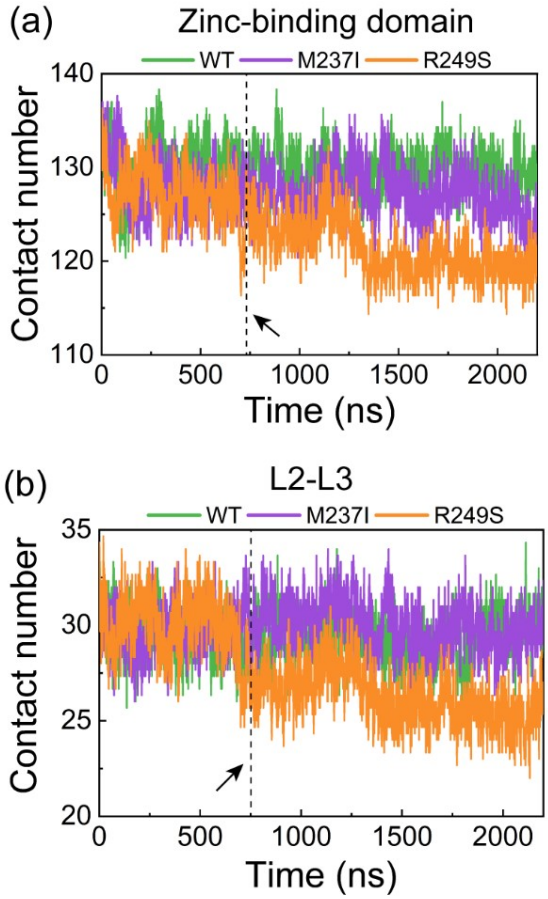

Fig. S5 Time evolution of contact number within zinc-binding domain (a) and that between L2 and L3 regions (b). The black dashed lines represent the time point at which the contact number begins to decrease in M237I and R249S p53C mutants.

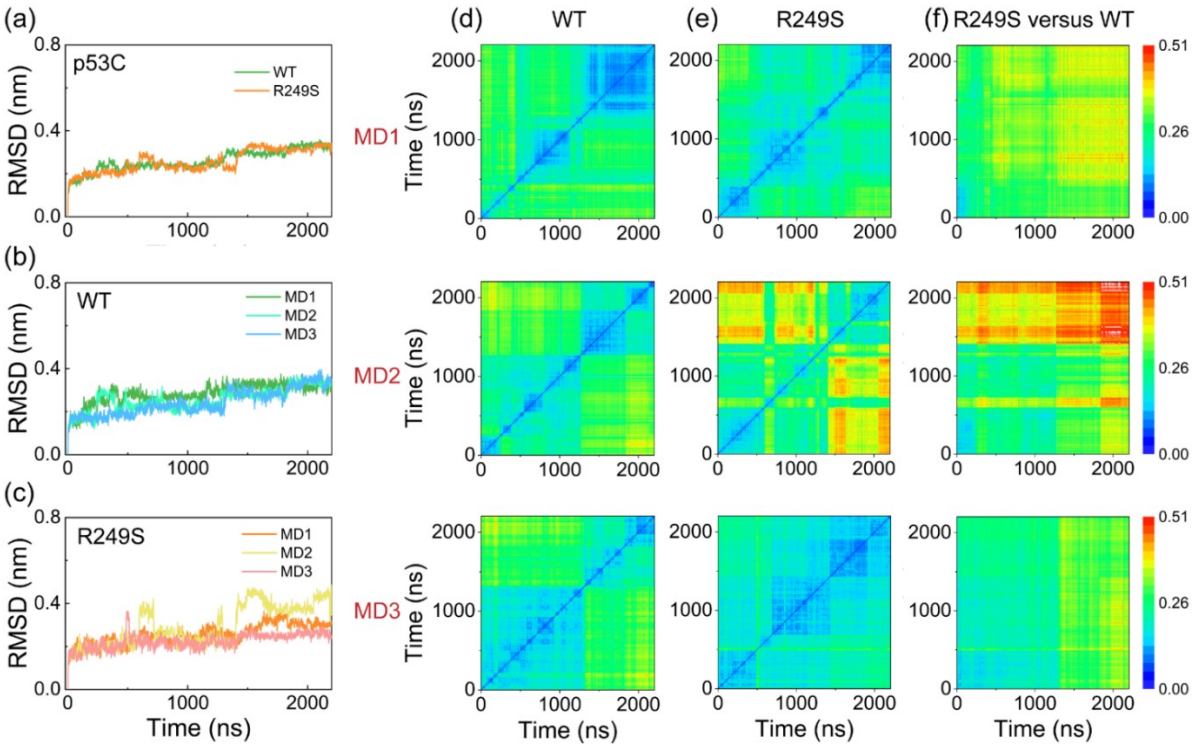

Fig. S6 (a-c) Time evolution of (a) backbone RMSD values of p53C averaged over three MD runs, (b) RMSD values of three WT MD runs, and (c) RMSD values of three R249S MD runs. (d-f) The RMSD values matrix of (d) WT, (e) R249S, and (f) R249S versus WT.

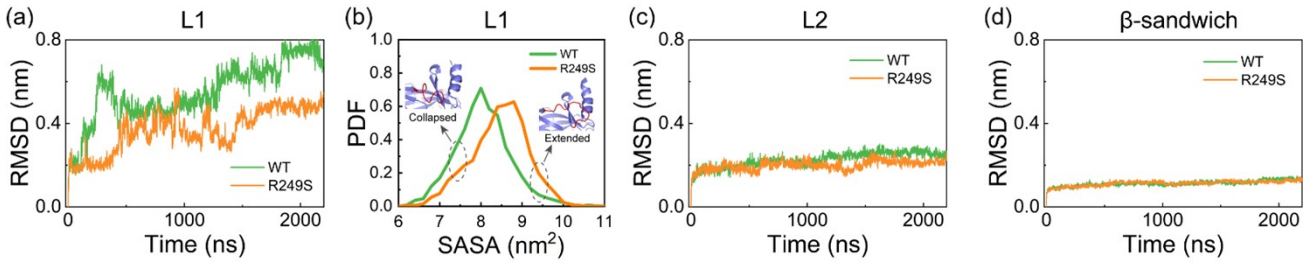

Fig. S7 (a) Time evolution of backbone RMSD values of loop L1 averaged over three MD runs. (b) PDF of the SASA value of loop L1, and the representative collapsed and extended states of loop L1 are shown. (c) Time evolution of backbone RMSD values of (c) loop L2 and (d) β-sandwich averaged over three MD runs.

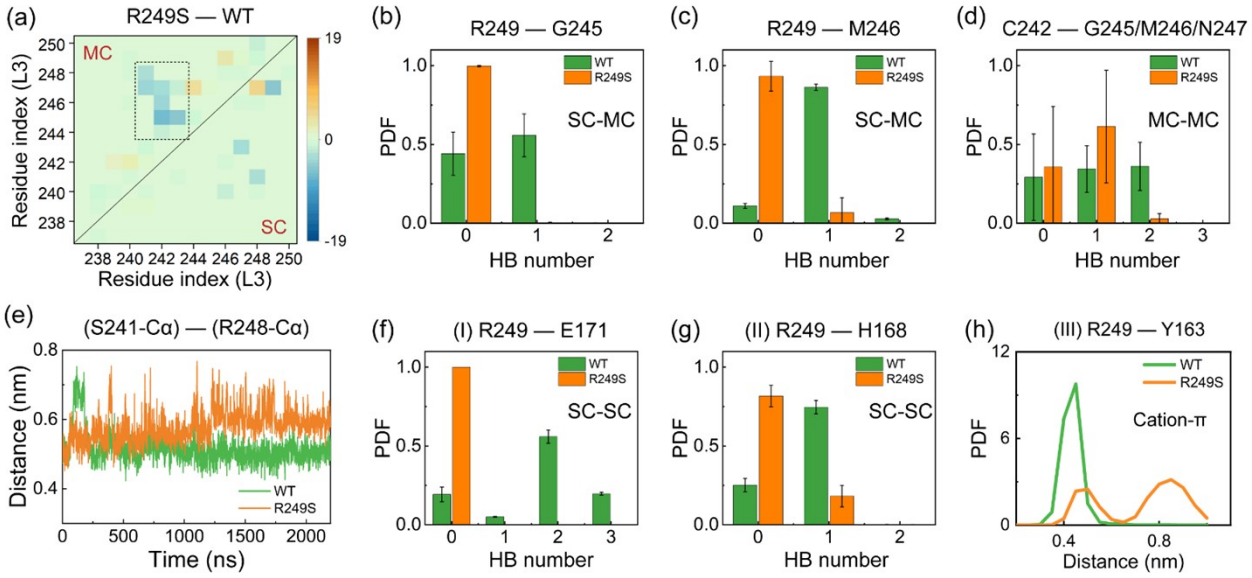

Fig. S8 (a) The differences of L3-L3 contact number map between R249S and WT (i.e. R249S minus WT, L3 residues: M237I-P250), the upper triangle region is the MC-MC interactions, the lower triangle region is the SC-SC interactions. (b-d) The PDF of HB number of residue pair (b) R/S249-G245, (c) R/S249-M246, and (d) C242-G245/M246/N247. (e) Time evolution of the distance between the Cα atom of residue S241 and the Cα atom of residue R248 in L3. (f-g) The PDF of HB number between residue pairs (f) R/S249-E171, SC-MC HB, and (g) R/S249-H168. (h) The PDF of distance of R/S249-Y163 cation-π interaction.

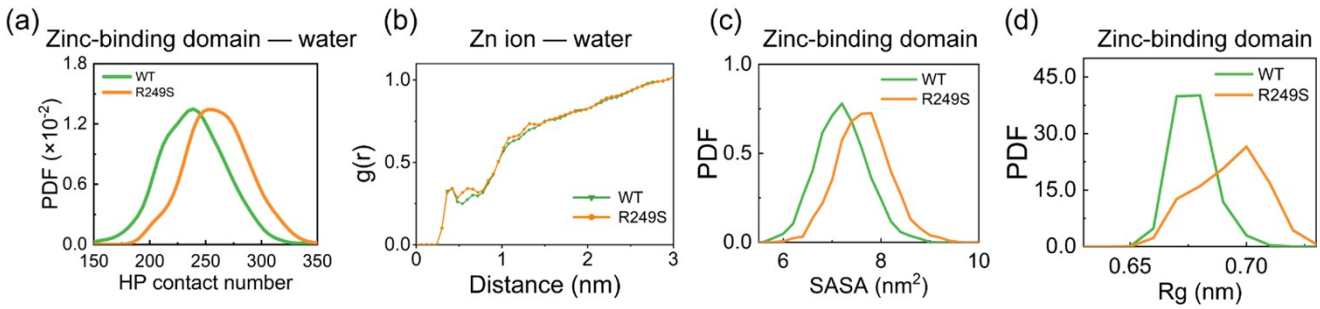

Fig. S9 (a) The PDF of hydrophobic contact number between zinc-binding domain and water molecules. (b) The RDF between the Zn ion in p53C and the oxygen atom in water molecules. (c-d) The PDF of the (c) SASA value and (d) Rg value of zinc-binding domain in p53C.

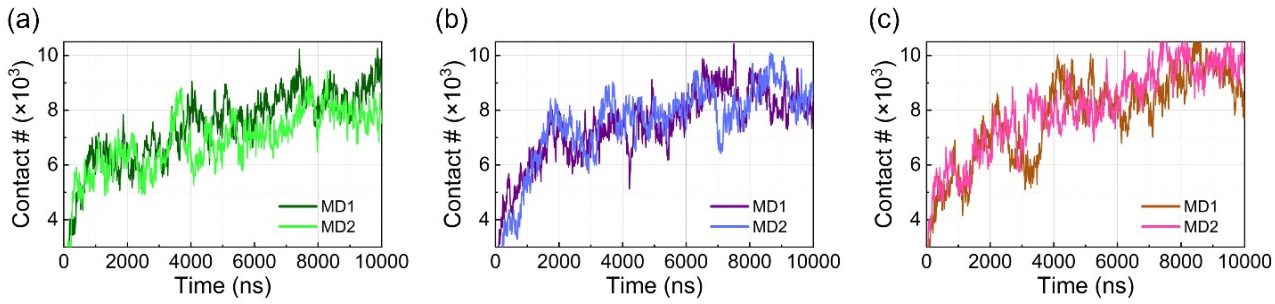

Fig. S10 (a-c) The time evolution of intermolecular contact number of WT (a), M237I (b), and R249S (c) p53C in each of the two individual MD trajectories at 37 ℃.

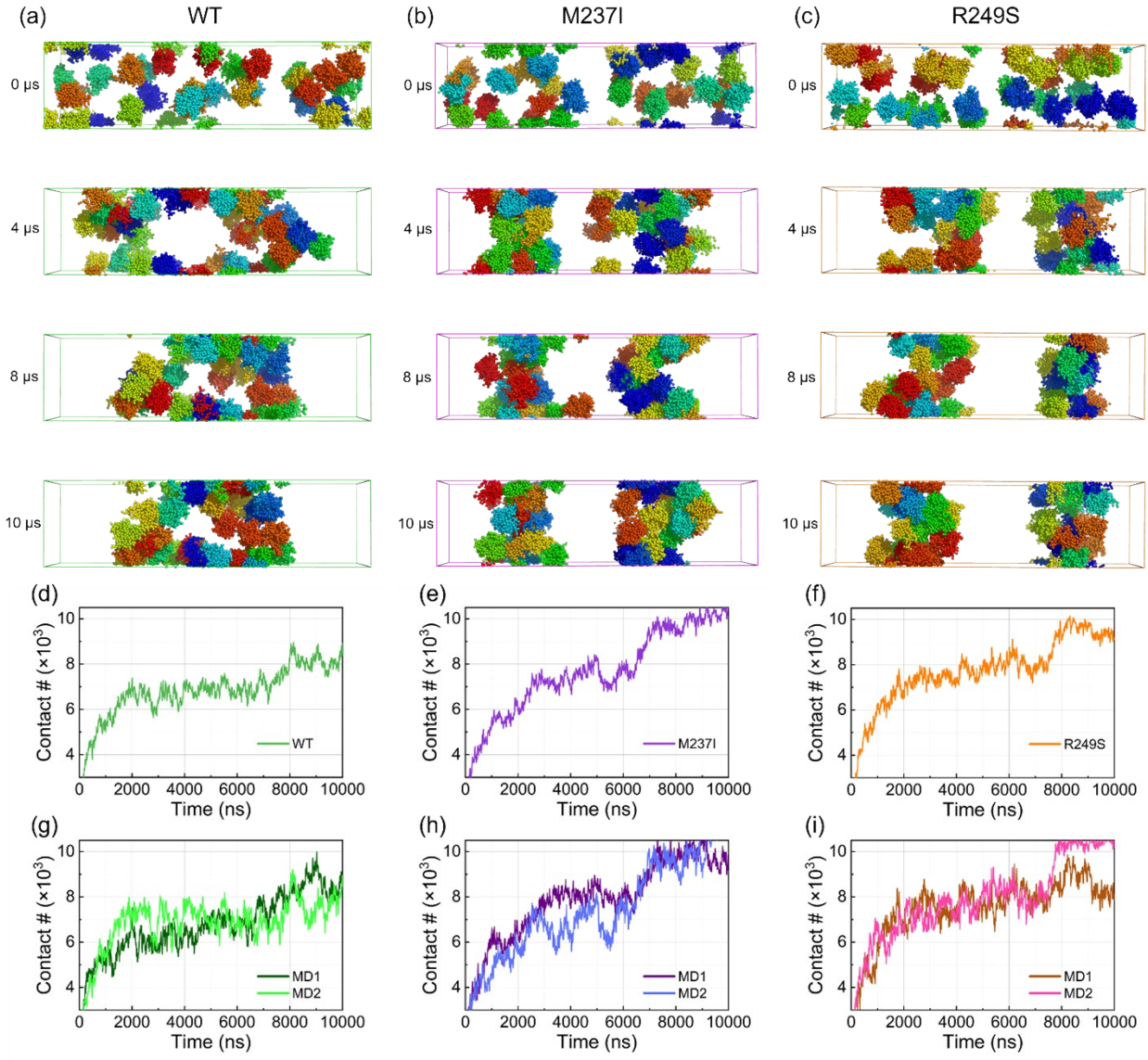

Fig. S11 Results of p53C phase separation simulations at 25 ℃. (a-c) Representative snapshots illustrating the LLPS process in WT (a), M237I (b), and R249S (c) p53C at four different time points in one MD simulation. (d-f) The time evolution of average intermolecular contact number over two individual trajectories for WT (d), M237I (e), and R249S (f) p53C. (g-i) Similar to (d-f), but for each of the two MD trajectories.

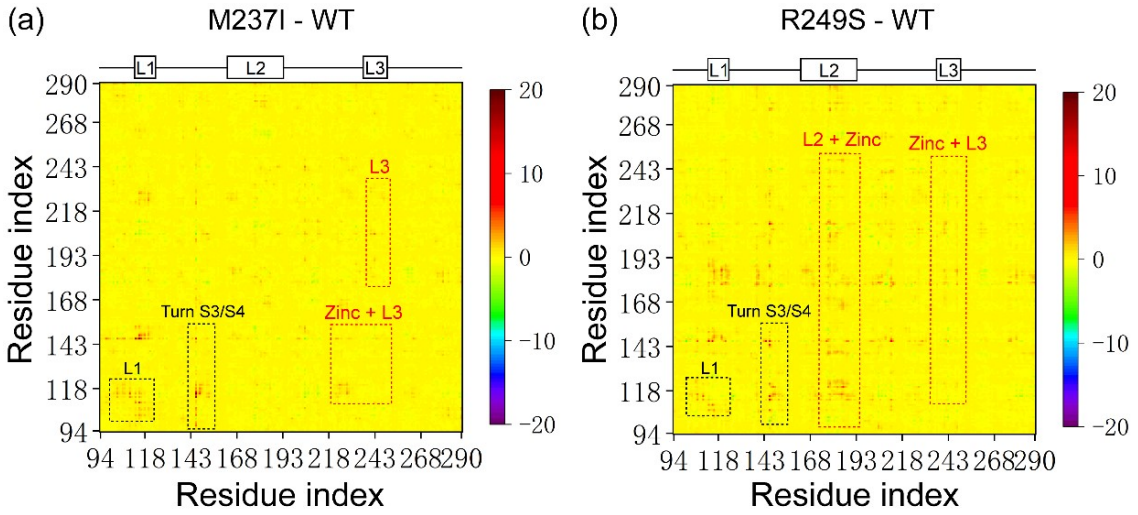

Fig. S12 (a) The differences of p53C residues contact number map between M237I and WT (i.e. M237I minus WT). (b) The differences of p53C residues contact number map between R249S and WT (i.e. R249S minus WT). The enhanced contacts are labeled by dashed rectangle and the red rectangle represents the regions consistent with the structural changes found in AA simulations ('Zinc' is short for zinc-binding domain, 'Turn S3/S4' is the turn structure between β-strand 3 and β-strand 4).

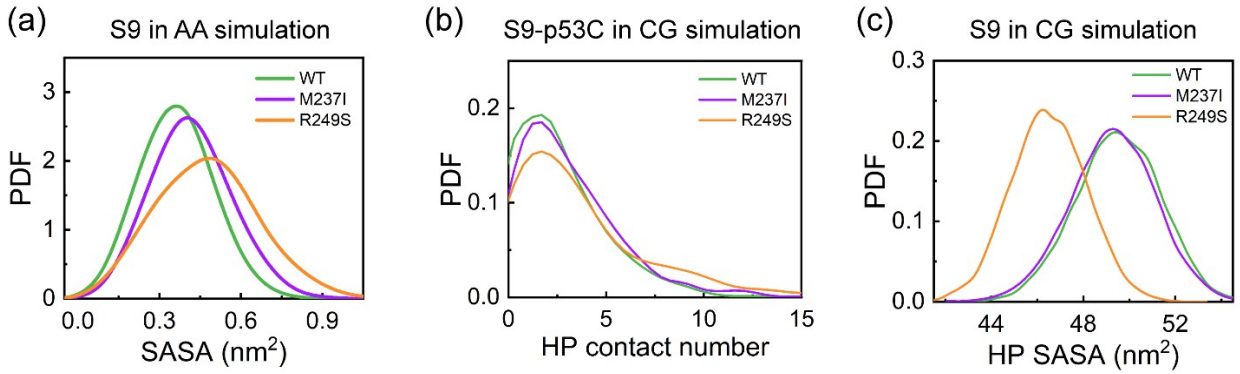

Fig. S13 (a) The PDF of SASA value of S9 segment (^{251}ILTIITL^{257}) in p53C AA simulations. (b) The PDF of hydrophobic contact number between S9 segments and p53C molecules. (c) The PDF of hydrophobic SASA value of S9 segments in p53C CG simulations.